Mitochondrial Free [Ca^{2+}] Increases during ATP/ADP Antiport and ADP Phosphorylation: Exploration of Mechanisms

Johan Haumann,[†] Ranjan K. Dash,[‡§] David F. Stowe,[†‡¶‖**] Age D. Boelens,[†] Daniel A. Beard,[‡§] and Amadou K. S. Camara[†*]

[†]Anesthesiology Research Laboratories, Department of Anesthesiology, [‡]Department of Physiology, [§]Biotechnology and Bioengineering Center, [¶]Cardiovascular Research Center, Medical College of Wisconsin, Milwaukee, Wisconsin; [‖]Department of Biomedical Engineering, Marquette University, Milwaukee, Wisconsin; and [**]Veterans Affairs Medical Center, Milwaukee, Wisconsin

ABSTRACT ADP influx and ADP phosphorylation may alter mitochondrial free [Ca^{2+}] ([Ca^{2+}]$_m$) and consequently mitochondrial bioenergetics by several postulated mechanisms. We tested how [Ca^{2+}]$_m$ is affected by $H_2PO_4^-$ (P_i), Mg^{2+}, calcium uniporter activity, matrix volume changes, and the bioenergetic state. We measured [Ca^{2+}]$_m$, membrane potential, redox state, matrix volume, pH_m, and O_2 consumption in guinea pig heart mitochondria with or without ruthenium red, carboxyatractyloside, or oligomycin, and at several levels of Mg^{2+} and P_i. Energized mitochondria showed a dose-dependent increase in [Ca^{2+}]$_m$ after adding $CaCl_2$ equivalent to 20, 114, and 485 nM extramatrix free [Ca^{2+}] ([Ca^{2+}]$_e$); this uptake was attenuated at higher buffer Mg^{2+}. Adding ADP transiently increased [Ca^{2+}]$_m$ up to twofold. The ADP effect on increasing [Ca^{2+}]$_m$ could be partially attributed to matrix contraction, but was little affected by ruthenium red or changes in Mg^{2+} or P_i. Oligomycin largely reduced the increase in [Ca^{2+}]$_m$ by ADP compared to control, and [Ca^{2+}]$_m$ did not return to baseline. Carboxyatractyloside prevented the ADP-induced [Ca^{2+}]$_m$ increase. Adding $CaCl_2$ had no effect on bioenergetics, except for a small increase in state 2 and state 4 respiration at 485 nM [Ca^{2+}]$_e$. These data suggest that matrix ADP influx and subsequent phosphorylation increase [Ca^{2+}]$_m$ largely due to the interaction of matrix Ca^{2+} with ATP, ADP, P_i, and cation buffering proteins in the matrix.

INTRODUCTION

Matrix free Ca^{2+} ([Ca^{2+}]$_m$) may play a major role in regulating mitochondrial function. Studies have shown a correlation between increased bioenergetics and increased [Ca^{2+}]$_m$ (1–6). However, excess [Ca^{2+}]$_m$ predisposes the mitochondria to form and open the permeability transition pore (mPTP) (7–11), a key factor in cell apoptosis; inhibition of mPTP formation reduces ischemia-reperfusion injury (12–17). The importance of [Ca^{2+}]$_m$ in both physiological and pathological conditions implies a necessity to tightly regulate [Ca^{2+}]$_m$.

[Ca^{2+}]$_m$ is regulated in part by voltage-dependent cation fluxes via a series of poorly identified cation channels and exchangers on the inner mitochondrial membrane (IMM) (7,8,10,18). The primary route for matrix Ca^{2+} uptake is via the ruthenium-red (RR)-sensitive Ca^{2+} uniporter (CU), whereas the principal Ca^{2+} efflux pathway is the Na^+/Ca^{2+} exchanger (NCE). There may also be Ca^{2+} efflux through a Na^+-independent Ca^{2+} exchanger (NICE), putatively a Ca^{2+}/H^+ exchanger (CHE) (19–22). Transport through the CU and NCE are dependent on the mitochondrial membrane potential ($\Delta\Psi_m$), whereas the CHE is thought to be concentration-, and not $\Delta\Psi_m$-dependent (21,23,24). Several independent studies have shown a correlation between a larger $\Delta\Psi_m$ and a higher [Ca^{2+}]$_m$ (10,22).

In measuring [Ca^{2+}]$_m$, we observed an increase in [Ca^{2+}]$_m$ with no added buffer $CaCl_2$ during state 3 respiration, a state in which $\Delta\Psi_m$ is decreased. This paradoxical increase in [Ca^{2+}]$_m$ implies a mechanism other than $\Delta\Psi_m$ in modulating [Ca^{2+}]$_m$. We tested five mechanisms that might play a role in this phenomenon:

The first mechanism that might explain an increase in [Ca^{2+}]$_m$ is allosteric activation of the CU by ADP to increase [Ca^{2+}]$_m$ (25). As ADP becomes phosphorylated, allosteric activation would decrease as [ADP] falls and [Ca^{2+}]$_m$ would return to the preexisting level. A second mechanism is that ADP phosphorylation might also induce a large matrix volume contraction, thereby raising [Ca^{2+}]$_m$.

A third possible mechanism is modulation of [Ca^{2+}]$_m$ by precipitation of free Ca^{2+} with P_i, such as $Ca_3(PO_4)_2$ (26). The complexing of Ca^{2+} with P_i is dependent on the product of concentrations of different species of P_i and Ca^{2+}. Thus, a decrease in matrix [P_i] would facilitate an increase in [Ca^{2+}]$_m$. In this situation, matrix [P_i] would be lower during state 3 respiration, as P_i becomes phosphorylated to ADP. After phosphorylation of ADP, matrix [P_i] would increase to near the level before phosphorylation, as Ca^{2+} would again form a complex with P_i.

A fourth possible mechanism is that the increased [Ca^{2+}]$_m$ results from basic physicochemical differences, i.e., different binding affinities (K_d) of ADP and ATP for Ca^{2+} (27). These differences in K_d predict an increase in [Ca^{2+}]$_m$ whenever the mitochondrial ADP/ATP ratio increases, and vice versa. Since ATP, ADP, and P_i bind variably to other cations (e.g., Mg^{2+} and H^+) as well, a change in concentration of these ions may also result in a significant change of free ATP, ADP, and P_i (ATP^{4-},

Submitted January 11, 2010, and accepted for publication April 28, 2010.

*Correspondence: aksc@mcw.edu

Editor: Ian Parker.

0006-3495/10/08/0997/10 $2.00

doi: 10.1016/j.bpj.2010.04.069

ADP^{3-}, and $H_2PO_4^-$) and thus alter the buffering capacity for Ca^{2+}.

A fifth possible mechanism is that the altered bioenergetic state during state 3 respiration leads to release of matrix Ca^{2+} stores by an unknown mechanism.

To explore which of these possible mechanisms might underlie the large change in $[Ca^{2+}]_m$ during transition to and from state 3 respiration, we measured matrix $[Ca^{2+}]_m$ as a function of extramatrix free $[Ca^{2+}]$ ($[Ca^{2+}]_e$) by increasing buffer $[CaCl_2]$. We also examined changes in $[Ca^{2+}]_m$ at a higher and lower buffer $[P_i]$ and $[Mg^{2+}]$, and assessed the effect of Δ[ADP] on matrix volume. Experiments were done with or without the CU blocker RR, the F_1F_0-ATPase blocker oligomycin (OMN), and the ADP/ATP carrier (AAC) blocker carboxy-atractyloside (CATR). Na^+/Ca^{2+} exchange (NCE) was inactive and was eliminated as a factor because there was no Na^+ present in the experimental buffer.

MATERIALS AND METHODS

Fluorescence measurements

Fluorescence spectrophotometry was used to measure matrix free Ca^{2+}, NADH, pH, and $\Delta\Psi_m$ (Qm-8, Photon Technology, Birmingham, NJ) (28–30). Isolated mitochondria (5 mg/ml) were incubated for 20 min at room temperature (25°C) with 5 μM indo-1 AM to measure $[Ca^{2+}]_m$ or with 5 μM BCECF AM to measure pH_m (Invitrogen, Carlsbad, CA) followed by suspension in 25 ml isolation buffer and repeated centrifugation at 8000 $\times$ *g*. The AM form of the dyes is taken up into the matrix where it is deesterified and retained. The dye-loaded pellet was resuspended in 0.5 ml isolation buffer, and protein concentration was measured again and diluted to 12.5 mg mitochondrial protein/ml. In other mitochondria, background autofluorescence (AF), which at 456 nm represents NADH (redox state), was measured and $\Delta\Psi_m$ was determined using rhodamine (Rh) 123. Mitochondria were kept on ice for the duration of the studies. All studies were conducted at room temperature. Please refer to the Supporting Material for detailed information on methods to assess matrix and extramatrix $[Ca^{2+}]_m$ and Mg^{2+}, redox state, matrix pH, $\Delta\Psi_m$, matrix volume, and respiration.

Experimental groups and protocol

Guinea pig heart mitochondria were isolated (see Supporting Material) as described previously (31,32) and diluted (33). Isolated mitochondria were divided into seven treatment groups: control (CON, 5 mM P_i), high P_i (HP, 10 mM P_i), low P_i (LP, 1 mM P_i), RR at start (RRS), RR later, after $CaCl_2$ addition (RRL), and OMN or CATR, each given at $t = -120$ s (Fig. 1). The CON mitochondria were suspended (0.5 mg/ml) in experimental buffer containing (in mM) 130 KCl (EMD Biosciences, San Diego, CA), 5 K_2HPO_4, 20 MOPS, 0.016 bovine serum albumin, and 0.04 EGTA, pH 7.15 (adjusted with KOH). To adjust for osmolarity, the HP and LP experimental buffers were adjusted to contain 123 mM KCl and 10 mM K_2HPO_4 (HP) or 136 mM KCl and 1 mM K_2HPO_4 (LP). MOPS, BSA, and EGTA concentrations and pH were the same for all groups. In the RRS group, 25 μM RR was added to the CON experimental buffer before energizing mitochondria. In the RRL group, 25 μM RR was added after the addition of $CaCl_2$. In the OMN and CATR groups, 100 μM OMN or 1.3 μM CATR was added before energizing mitochondria. In selected studies, 1 mM $MgCl_2$ was present while the $CaCl_2$ and ADP were added (see Supporting Material).

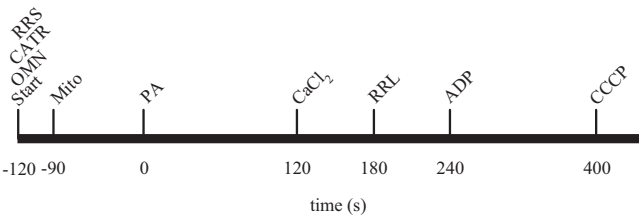

FIGURE 1 Time line for adding substances to experimental buffer. *PA*, pyruvic acid; *RRS* and *RRL*, ruthenium red at start or later; *ADP*, adenosine diphosphate; *CATR*, carboxyatractyloside; *OMN*, oligomycin; *CCCP*, carbonylcyanide m-chlorophenylhydrazone.

Experiments were initiated at $t = -120$ s, when OMN, CATR, and RR were added to comprise the OMN, CATR, and RRS groups; at $t = -90$ s, mitochondria were added (Fig. 1). At $t = 0$ s, pyruvic acid (PA, 0.5 mM) was added, followed by either of two concentrations of $CaCl_2$ (10 or 25 μM in deionized H_2O) or vehicle (0 $CaCl_2$) at $t = 120$ s. At $t = 180$ s, RR was added to the RRL group. At $t = 240$ s, ADP (250 μM) was added, followed by 4 μM of the protonophore carbonylcyanide m-chlorophenylhydrazone (CCCP) at $t = 400$ s to maximally depolarize the IMM. All buffers and reagents, including substrates, were Na^+-free to prevent NCE activation. Inactivity of the NCE was verified by comparing data from experiments with and without added CGP-37157, a specific mitochondrial NCE inhibitor (data not shown). When no drug or $CaCl_2$ was added, the appropriate vehicle was added to the mitochondrial suspension. All chemicals were obtained from Sigma-Aldrich (St. Louis, MO) unless noted otherwise.

Statistical analyses

All data are presented as the mean $\pm$ SE. Repeated-measures ANOVA followed by a post hoc analysis using Student-Newman-Keuls' test was performed to determine statistically significant differences between and within groups. Data for analysis were collected at the times noted above. A *P* value of <0.05 (two-tailed) was considered significant.

RESULTS

Extramatrix and matrix free $[Ca^{2+}]$ and inhibition of CU

Adding 0, 10, or 25 μM $CaCl_2$ to the mitochondrial suspension caused a rapid, concentration-dependent increase in $[Ca^{2+}]_e$ to initial values of 20 $\pm$ 3, 114 $\pm$ 13, and 485 $\pm$ 40 nM (Fig. 2) due to the presence of 40 μM of EGTA. This was followed by a slower, steady decline in $[Ca^{2+}]_e$ as Ca^{2+} was transported into mitochondria via the CU; this was most prominent after adding 25 μM $CaCl_2$. Transport of Ca^{2+} through the CU was confirmed in the RR groups because RR blocked the subsequent decrease in $[Ca^{2+}]_e$. Adding ADP did not significantly affect $[Ca^{2+}]_e$ in the absence of RR. In the presence of RR there was a significant decrease in $[Ca^{2+}]_e$ when ADP was added.

Adding $CaCl_2$ caused a concentration-dependent increase in matrix $[Ca^{2+}]_m$ (Fig. 3), which took place via the CU, as verified again by the nearly complete block in response to RR (Fig. 3 *C*). After adding 10 μM $CaCl_2$ (initially equivalent to 114 nM $[Ca^{2+}]_e$), $[Ca^{2+}]_m$ increased from 80 $\pm$ 5 nM to 183 $\pm$ 7 nM. After adding 25 μM $CaCl_2$ (initially

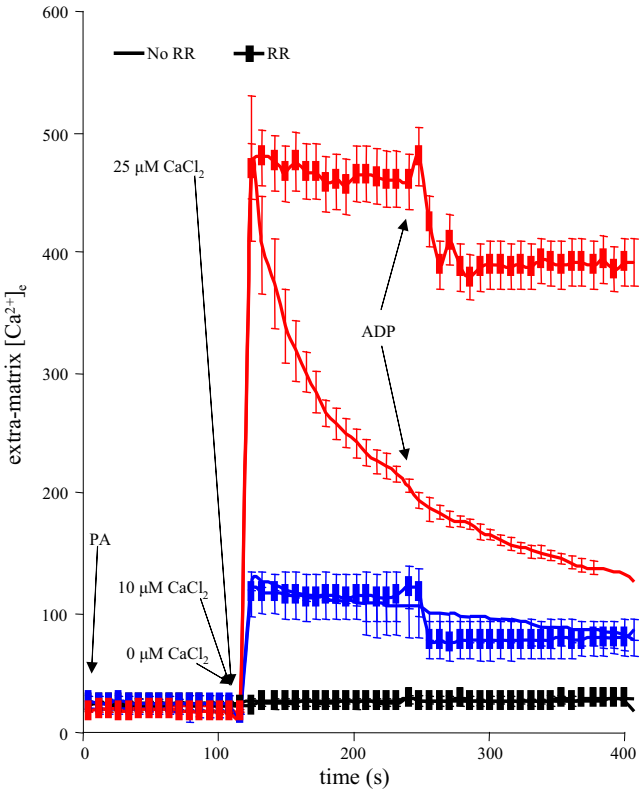

FIGURE 2 Extramatrix free $[Ca^{2+}]$ ($[Ca^{2+}]_e$) over time measured using indo-1 (in the presence of 40 μM EGTA). Adding $CaCl_2$ increased $[Ca^{2+}]_e$ in a concentration-dependent manner. Adding 25 μM $CaCl_2$ increased $[Ca^{2+}]_e$ up to 485 nM, which then slowly declined as Ca^{2+} was taken up into the matrix. Adding 10 μM $CaCl_2$ increased $[Ca^{2+}]_e$ to 114 nM with a lesser and slower subsequent Ca^{2+} uptake. RR blocked matrix uptake of Ca^{2+} through the CU so that $[Ca^{2+}]_e$ remained constant. ADP caused a small decrease in $[Ca^{2+}]_e$ only in the presence of RR.

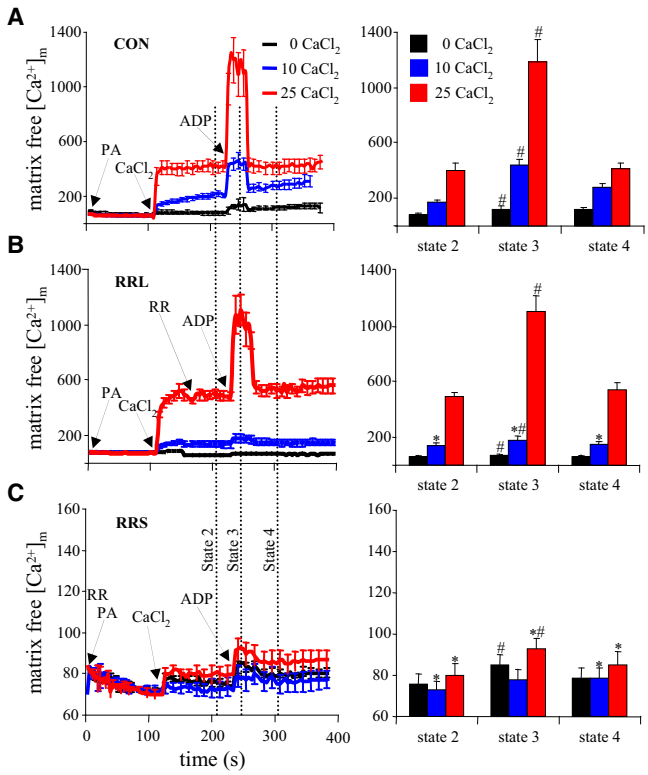

FIGURE 3 Effects of ADP and RR on $[Ca^{2+}]_m$ over time, measured using indo-1 AM. Dynamic, time-dependent changes (*left column*) and mean changes (*right column*) taken at the vertical dotted lines in the left column are displayed. (*A*) Adding 10 and 25 μM $CaCl_2$ in energized mitochondria (after PA) caused abrupt, graded increases in $[Ca^{2+}]_m$ to steady-state values. Adding ADP caused an abrupt but transient rise in $[Ca^{2+}]_m$ above the values established with added $CaCl_2$. (*B*) Adding RR after 25 μM $CaCl_2$ (RRL) did not blunt the rise in $[Ca^{2+}]_m$ induced by adding ADP. (*C*) Adding RR before $CaCl_2$ (RRS) blocked Ca^{2+} uptake, but the ADP-induced increase in $[Ca^{2+}]_m$ remained evident, although it was much smaller (note scale) after adding 25 μM $CaCl_2$. In the right column, for $P < 0.05$, # indicates state 3 versus states 2 and 4 respiration; * indicates RRL and RRS versus the CON group at the same respiration state and $CaCl_2$.

equivalent to 485 nM $[Ca^{2+}]_e$), $[Ca^{2+}]_m$ increased from 80 ± 5 to 518 ± 44 nM. Note that $[Ca^{2+}]_m$ (Fig. 3) remained at a steady-state level, whereas $[Ca^{2+}]_e$ (Fig. 2) continued to decrease in the CON group from its initial value of 485 nM $[Ca^{2+}]$ (after adding 25 μM $CaCl_2$).

Adding ADP caused a proportional increase in $[Ca^{2+}]_m$ in the CON, RRS, and RRL groups (Fig. 3), i.e., the magnitude of increase was dependent on the $[Ca^{2+}]_m$ before ADP was added. The effect of ADP was absent in the RR group with 10 μM added $CaCl_2$, as $[Ca^{2+}]_m$ was low (80 ± 5 nM). ADP addition increased $[Ca^{2+}]_m$ only a little (Fig. 3 *C*), probably because adding $CaCl_2$ after RR did not increase $[Ca^{2+}]_m$. The effect of ADP on increasing $[Ca^{2+}]_m$ was similar in the RRL and CON groups and smaller in the RRS group after adding $CaCl_2$. There was an attenuated increase of $[Ca^{2+}]_m$ (25 μM Ca^{2+}; 485 nM $[Ca^{2+}]_e$), though not a significant one, in the RRL versus the CON group. Matrix uptake of Ca^{2+} continued in the CON group. Adding RR after 180 s stopped this slow uptake, resulting in a smaller increase in $[Ca^{2+}]_m$ after adding 10 μM (114 nM $[Ca^{2+}]_e$). However, extending the time of Ca^{2+} uptake before adding RR in the 10-μM group resulted in an increase in $[Ca^{2+}]_m$ beyond 180 s similar to that of the CON group. Adding ADP after RR then increased $[Ca^{2+}]_m$ as much as in the CON group (data not shown).

$[Ca^{2+}]_m$ increased as a function of $[Ca^{2+}]_e$, and this was attenuated during state 3 respiration (Fig. 4). These data show that $[Ca^{2+}]_m$ reached a value twofold higher than that of $[Ca^{2+}]_e$ at $t = 180$ s (state 2 respiration). $[Ca^{2+}]_m$ was 80 ± 5, 212 ± 10, and 518 ± 44 nM, whereas $[Ca^{2+}]_e$ was 26 ± 3, 112 ± 12, and 266 ± 12 nM after adding 0, 10, and 25 μM $CaCl_2$. This plot also shows that $[Ca^{2+}]_m$ increased 1.75- and twofold during state 3 versus state 2 respiration (from 518 ± 44 nM to 1039 ± 83 nM), whereas $[Ca^{2+}]_e$ decreased slightly. These data support the proposal that as more Ca^{2+} becomes buffered in the matrix after $CaCl_2$ addition, some is released during ADP/ATP antiport and ADP phosphorylation, possibly due to

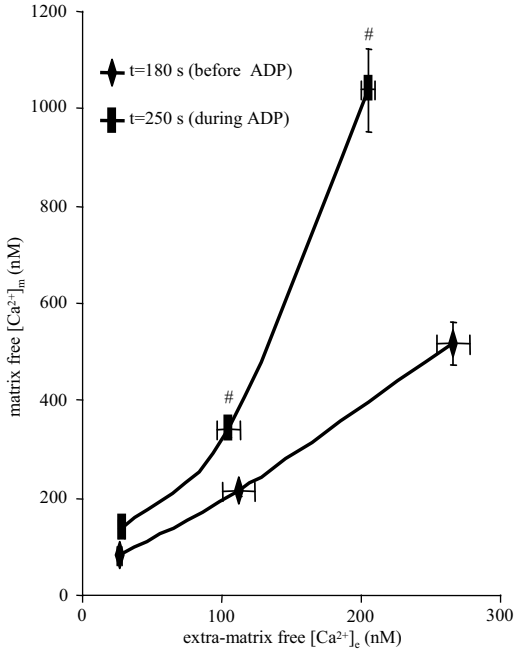

FIGURE 4 $[Ca^{2+}]_m$ as a function of $[Ca^{2+}]_e$. $[Ca^{2+}]_e$ and $[Ca^{2+}]_m$ were measured at $t = 100$ s (before added $CaCl_2$), at $t = 180$ s (after added $CaCl_2$), and at $t = 250$ s (in the presence of ADP). ADP caused a more than additive increase in $[Ca^{2+}]_m$ as a function of $[Ca^{2+}]_e$, and the increase was dependent on the existing $[Ca^{2+}]_m$ level. Data were taken from Figs. 2 and 3 *A*. For $P < 0.05$, # indicates state 3 versus states 2 and 4 respiration.

a decrease in matrix Ca^{2+} buffering sites (e.g., ADP, proteins).

Effect of buffer P_i and Mg^{2+} on matrix free $[Ca^{2+}]$

The effect on $[Ca^{2+}]_m$ of altering buffer $[P_i]$ was evaluated at different $[CaCl_2]_e$ and during ADP addition (Fig. 5). Buffer [KCl] was adjusted against $[K_2HPO_4]$ to maintain the same osmolarity. With no added $CaCl_2$, there were no detectable changes in $[Ca^{2+}]_m$ among the three $[P_i]$ groups. A change in buffer $[P_i]$ from 5 to 1, and from 5 to 10 mM, did not significantly affect $[Ca^{2+}]_m$ after adding $CaCl_2$; however, at 25 μM $CaCl_2$ and 1 mM $[P_i]$ (LP), the initial (fast) uptake of Ca^{2+} was followed by a slow decrease in $[Ca^{2+}]_m$. The increase in $[Ca^{2+}]_m$ after adding ADP did not differ among the P_i groups.

In a few studies, 1 mM $MgCl_2$ was added to the buffer (Fig. S1 *A* in the Supporting Material). Calculated matrix $[Mg^{2+}]$ (see Supporting Material, Methods) was 0.51 $\pm$ 0.03 mM without added $MgCl_2$ and 0.85 $\pm$ 0.02 mM after adding 1 mM $MgCl_2$ to the buffer. In the presence of $MgCl_2$ the same amount of added $CaCl_2$ resulted in a lesser rise in $[Ca^{2+}]_m$; however, adding ADP caused a proportional increase in $[Ca^{2+}]_m$ when more $CaCl_2$ was added to the buffer to counter the Mg^{2+}-inhibited transport of Ca^{2+} through the CU (Fig. S1 *A*).

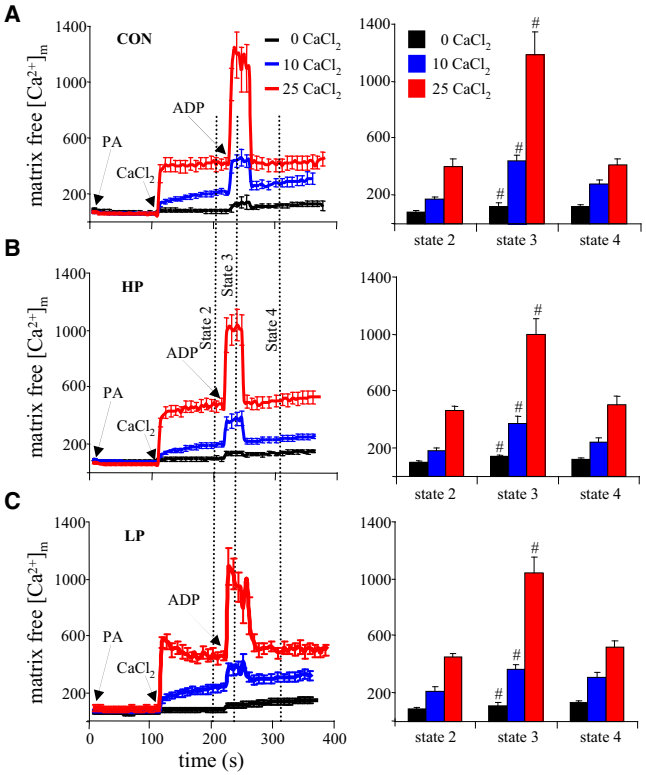

FIGURE 5 Effects of ADP and altered buffer P_i on $[Ca^{2+}]_m$. (*A*) Same as Fig. 3 *A*, where $[P_i]$ is 5 mM. (*B*) In both the 10-mM and 1-mM $[P_i]$ groups, there were no significant differences in response to added $CaCl_2$ or ADP versus the corresponding 5-mM $[P_i]$ group. For $P < 0.05$, # indicates state 3 versus states 2 and 4 respiration; * indicates the HP and LP versus CON groups at the same respiration state and $CaCl_2$. See Fig. 3 legend for additional details.

Effect of ADP versus ATP on mitochondrial matrix volume versus $[Ca^{2+}]$

Added ADP resulted in a transient volume decrease of 7% (photon count) with a corresponding 51% increase in $[Ca^{2+}]_m$ in the 25 μM $CaCl_2$ group, whereas the maximal volume increase after valinomycin (VAL) was 52% with a corresponding decrease in $[Ca^{2+}]_m$ after VAL of only 18% (Fig. S1 *B*). The ratio of volume to $[Ca^{2+}]_m$ during responses to VAL over ADP—(52/18) divided by (7/51) = 0.05—indicated that this small decrease in volume caused by addition of ADP could account for only ~5% of the increase in $[Ca^{2+}]_m$.

Effect of blocking ADP and ATP transport on matrix free $[Ca^{2+}]$

Mitochondria were treated with OMN or CATR, which inhibit the F_1F_0-ATPase and the AAC respectively, to evaluate the effect of the organic phosphates ADP and ATP on $[Ca^{2+}]_m$. In the presence of OMN, $[ADP]_m$ and $[ATP]_m$ change when ADP is added, because ATP is exchanged for ADP at the AAC. With blocked phosphorylation of

ADP by OMN, matrix $[P_i]$ is expected to remain unchanged. In the presence of CATR, however, there can be no changes in $[ADP]_m$ or $[ATP]_m$ during added buffer ADP, because the AAC is blocked.

OMN and CATR had no effect on $[Ca^{2+}]_m$ when 0, 10, or 25 μM $CaCl_2$ was added; thus, there was no effect of these drugs on matrix Ca^{2+} uptake (Fig. 6), but the response to ADP after OMN was a small but significant increase in $[Ca^{2+}]_m$. Moreover, this increase in $[Ca^{2+}]_m$ was sustained beyond the period when ADP would have been completely phosphorylated. This increase in $[Ca^{2+}]_m$ may indicate limited ADP entry into the matrix in exchange for ATP efflux. The $[Ca^{2+}]_m$ response to ADP was abolished after CATR as both ATP efflux and ADP influx were blocked.

Effect of increasing $[Ca^{2+}]_m$ on the NADH redox state

PA increased NADH in all groups. Adding either 10 or 25 μM $CaCl_2$ did not change NADH compared to vehicle (CON, Fig. 7 *A*). Adding ADP caused a transient and reversible oxidation of NADH (i.e., a decrease in signal) in all groups, except in the OMN and CATR groups (data not shown), because ADP transport and phosphorylation were blocked in these groups. NADH returned to pre-ADP levels as ADP was phosphorylated to ATP. The presence of RR or a different $[P_i]$ did not affect redox state (data not shown).

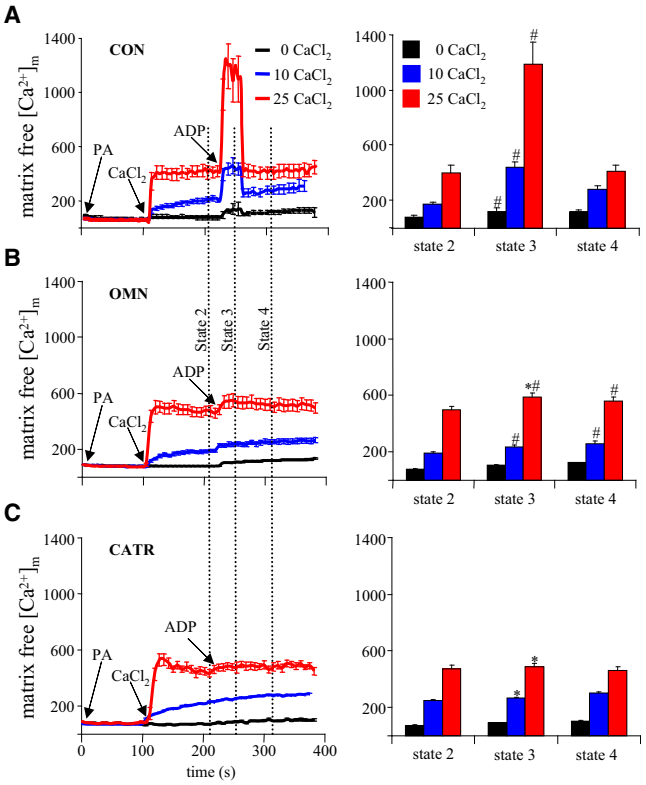

FIGURE 6 Effect of ADP on $[Ca^{2+}]_m$ during inhibited phosphorylation and blocked ADP/ATP transport. (*A*) Same as Fig. 3 *A*. (*B*) Adding ADP after $CaCl_2$ and blocking F_1F_0-ATPase with OMN caused a significant increase in $[Ca^{2+}]_m$ after addition of both 10 and 25 μM $CaCl_2$. (*C*) Adding ADP after $CaCl_2$ when the ADP/ATP carrier was blocked with CATR inhibited the ADP-induced increase in $[Ca^{2+}]_m$. For $P < 0.05$, # indicates state 3 versus states 2 and 4 respiration; * indicates the OMN and CATR versus CON groups at the same respiration state and $CaCl_2$. See Fig. 3 for additional details.

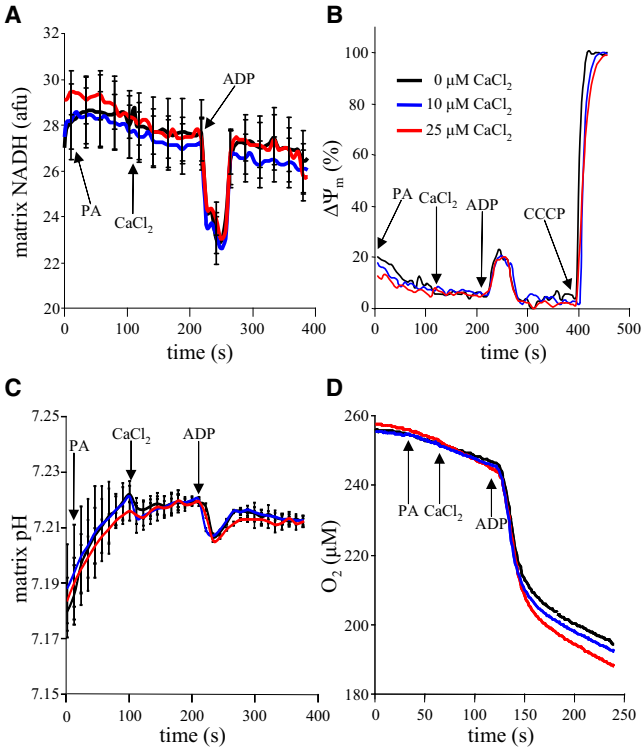

FIGURE 7 Effects of adding $CaCl_2$ and ADP on mitochondrial bioenergetics. All data correspond to $[Ca^{2+}]_m$ data displayed in Fig. 3 *A* (CON). (*A*) PA increased NADH as the TCA cycle was activated. Adding $CaCl_2$ did not significantly alter NADH values. (*B*) ADP transiently oxidized mitochondria (i.e., reduced NADH (*A*)) as energy contained in $\Delta\Psi_m$ was consumed, as shown by the transiently lowered $\Delta\Psi_m$. (*C*) PA induced a mild alkalinization; adding $CaCl_2$ did not further alter the matrix pH. ADP transiently reduced matrix pH as matrix proton influx temporarily exceeded proton pumping. (*D*) O_2 consumption (respiration) increased on addition of PA, and more so on addition of 25 μM $CaCl_2$. Adding ADP markedly enhanced O_2 consumption, but adding $CaCl_2$ did not produce any additional effect on respiration. See Table 1 for summary data and statistics on respiration.

Effect of increasing $[Ca^{2+}]_m$ on $\Delta\Psi_m$

Energizing mitochondria with PA increased $\Delta\Psi_m$ in all groups. Adding $CaCl_2$ had no significant effect on $\Delta\Psi_m$ (CON, Fig. 7 *B*). Adding ADP caused a transient and reversible partial depolarization of $\Delta\Psi_m$ in all groups, as ADP was transported into the matrix and phosphorylated to ATP, which was also not affected by added $CaCl_2$. $\Delta\Psi_m$ was not affected by RR or at different buffer $[P_i]$ or $[Mg^{2+}]$ (data not shown). The ADP-induced depolarization did not occur when ADP and ATP transport was prevented

by CATR or when phosphorylation of ADP to ATP was blocked by OMN (data not shown). CCCP maximally depolarized the IMM.

Effect of increasing $[Ca^{2+}]_m$ on matrix pH

Matrix pH increased on energizing mitochondria with PA. Adding $CaCl_2$ had no significant effect on matrix pH compared to vehicle (CON, Fig. 7 *C*). Adding ADP acidified the matrix as protons enter the matrix through the F_1F_0ATP-ase to generate ATP. This alteration in pH by ADP was not affected by adding RR or by altering buffer $[P_i]$, but was inhibited by CATR or OMN (data not shown). Adding CCCP caused matrix acidification, as this protonophore facilitates transport of protons across the IMM (data not shown).

Effect of increasing $[Ca^{2+}]_m$ on respiration

Respiration rates in states 2 and 4 were significantly increased only at 518 nM $[Ca^{2+}]_m$ (Fig. 7 *D* and Table 1); state 3 respiration was higher but unaltered at any $[Ca^{2+}]_m$. At 183 nM $[Ca^{2+}]_m$, respiration rates in states 2 and 4 were not significantly altered. Therefore, the respiratory control index (RCI) remained unchanged at 183 nM $[Ca^{2+}]_m$, and slightly decreased at 518 nM $[Ca^{2+}]_m$, due to the change in state 4 respiration. Adding $MgCl_2$ had no added effect on state 3 or state 4 respiration (Fig. S1 *C*). Respiratory effects of $[Ca^{2+}]_m$ were also not altered at any $[P_i]$ (data not shown).

DISCUSSION

Changes in matrix free $[Ca^{2+}]_m$ during respiration

This study demonstrates that in energized heart mitochondria, a transient ADP influx coupled to instantaneous ATP efflux markedly increases $[Ca^{2+}]_m$. Moreover, this study demonstrates that acute physiological changes in $[Ca^{2+}]_m$ have little effect on mitochondrial bioenergetics other than to slightly increase resting-state respiration. The ADP-induced rise in $[Ca^{2+}]_m$ may be in large part due either to the lower Ca^{2+} buffering capacity of ADP versus ATP or to an ADP-induced protein release of stored matrix Ca^{2+}. This transient increase in $[Ca^{2+}]_m$ is not measurably altered by Mg^{2+} or $P_{i,}$, and is little affected by an ADP-induced matrix contraction, or by ADP-induced uptake of matrix Ca^{2+} via the CU.

TABLE 1 O_2 consumption in different respiratory states

	State 2	State 3	State 4	RCI
0 $CaCl_2$	0.91 ± 0.04	14.07 ± 0.58	1.01 ± 0.05	13.6 ± 0.41
10 $CaCl_2$	0.87 ± 0.04	14.15 ± 0.58	1.08 ± 0.02	13.0 ± 0.36
25 $CaCl_2$	1.04 ± 0.03*	14.44 ± 0.48	1.19 ± 0.02*	12.1 ± 0.28*

Oxygen consumption was measured in μmol O_2/h/mg protein. Adding $CaCl_2$ (485 nM $[Ca^{2+}]_e$) significantly increased O_2 uptake in states 2 and 4 and lowered RCI (state 3/state 4 ratio).

The uptake of $[Ca^{2+}]_m$ at a given $[Ca^{2+}]_e$ (Fig. 4) supports earlier studies (34,35) showing that Ca^{2+} influx through the CU causes Ca^{2+} to accumulate in the matrix, as predicted by the Nernst equation. However, the twofold gradient between $[Ca^{2+}]_m$ and $[Ca^{2+}]_e$ observed in this study after adding $CaCl_2$ (114 or 485 nM $[Ca^{2+}]_m$) is smaller than that reported in earlier studies (34,35). Differences in species, isolation techniques, energy state, buffering capacities, equilibration rate, and measurement and calibration techniques for ionized $[Ca^{2+}]$ could underlie some of the differences.

The small, steady decline in $[Ca^{2+}]_e$ after addition of ADP (Fig. 2) could be due to increased sequestration of matrix free Ca^{2+} by matrix proteins. The continuous decrease in $[Ca^{2+}]_e$ without any further change in $[Ca^{2+}]_m$ after a rapid rise in $[Ca^{2+}]_m$ upon addition of 25 μM $CaCl_2$ to the buffer (485 nM $[Ca^{2+}]_e$) is an interesting phenomenon that might also be explained by accumulating matrix Ca^{2+} storage in the form of Ca-PO_4 complexes (26), such as $Ca_3(PO_4)_2$, as Ca^{2+} enters the matrix through the CU. Formation of these complexes could result in a steady-state $[Ca^{2+}]_m$ during continued matrix Ca^{2+} uptake, as additional Ca^{2+} entering the matrix will precipitate with PO_4^{3-}. Although there is no direct evidence for matrix Ca-PO_4 complex formation, there are indications that it occurs (36–38). However, we could not observe a clear difference in $[Ca^{2+}]_m$ at different buffer $[P_i]$, perhaps because of the low, but physiologic, $[Ca^{2+}]_m$.

Adding ADP at any $[Ca^{2+}]_m$ caused a further 1.6- to 2-fold increase in $[Ca^{2+}]_m$ during state 3 compared to state 2 respiration (Fig. 4). This effect of ADP on $[Ca^{2+}]_m$ was more than additive at higher $[Ca^{2+}]_m$ and is unlikely to be due to activation of the CU by ADP because the ADP-induced increases in $[Ca^{2+}]_m$ were not appreciably reduced by RR (Fig. 3). Although ADP transiently reduced matrix volume, this was not in itself sufficient to account for the much larger increases observed in $[Ca^{2+}]_m$. Further, it is possible that a change in light scattering during state 3 respiration may also arise from a change in mitochondrial shape. Overall, these data suggest that matrix contraction by ADP is not an important factor.

There was no clear correlation among the different buffer $[P_i]$s and increases in $[Ca^{2+}]_m$ on ADP addition. The relationship between $[Ca^{2+}]_m$ and $[P_i]$ has been shown previously (26), although at a relatively high $[Ca^{2+}]_m$, and that study did not examine for any difference in $[Ca^{2+}]_m$ during state 3 respiration. It was not feasible to use P_i carrier blockers in our experiments to examine the importance of matrix $[P_i]$ on $[Ca^{2+}]_m$ during state 3 respiration, because these blockers affect ADP/ATP transport as well (39).

In contrast to $[P_i]$, the differential binding of ADP and ATP to Ca^{2+} apparently plays an important role in the ADP-induced increase in $[Ca^{2+}]_m$, as shown by the slight increase of $[Ca^{2+}]_m$ in the OMN versus the CATR group. The lack of an increase in $[Ca^{2+}]_m$ on ADP addition after

blocking the AAC shows that the ADP-induced increase in $[Ca^{2+}]_m$ is not due to contamination of ADP with divalent cations that can bind to indo-1. The small but significant increase in $[Ca^{2+}]_m$ in the OMN group shows that a change in $[ADP]_m$, without altering matrix $[P_i]$, can change $[Ca^{2+}]_m$. As discussed below, ADP binds to Ca^{2+} with a 10-fold lower affinity than does ATP; therefore, a decrease in matrix ATP due to ADP/ATP exchange alone may explain some of the increase in $[Ca^{2+}]_m$. Another possible explanation for the ADP effect is release of ionized Ca^{2+} from proteins similar to calsequestrin, a release mechanism that is observed in the sarcoplasmic reticulum (40).

To better understand how ATP, ADP, and P_i affect $[Ca^{2+}]_m$, it is first necessary to understand how these molecules are taken up into mitochondria and how they differentially bind to Ca^{2+}. ADP^{3-} enters mitochondria via the AAC in exchange for ATP^{4-}. Since this transport is electrogenic, and constitutes a net influx of one positive charge, it is driven by, and uses the energy of, the $\Delta\Psi_m$ (41–43). In the matrix, ADP is phosphorylated to ATP by the F_1F_0ATP-ase, a process driven by proton flux into the matrix. The P_i carrier is responsible for electroneutral cotransport of P_i^-/H^+ (or P_i^-/OH^- antiport), which is driven by the proton gradient, ΔpH (44–46).

Phosphorylation of ADP and dephosphorylation of ATP are dependent on the mitochondrial bioenergetic state (e.g., ΔpH) and ATP utilization by the cell, respectively. ADP levels rise in the matrix when extramatrix ADP is added and the ATP that is formed is ejected rapidly from the matrix by the AAC; matrix ADP levels remain elevated until all ADP is phosphorylated to ATP (4,47). It is important to note that the dissociation constants (K_ds) for ATP and ADP (Table S1) indicate a 10-fold greater binding affinity of Ca^{2+} and Mg^{2+} with ATP^{4-} over ADP^{3-}, and a twofold greater binding affinity of Mg^{2+} versus Ca^{2+} to these phosphates. The binding affinities of these phosphate entities are uniformly high for H^+ and very low for K^+. Our premise is that these differences in binding affinities for ATP and ADP largely account for the ADP-induced increase in $[Ca^{2+}]_m$.

The results of these experiments imply a small role for P_i and a larger role for the ADP/ATP ratio in buffering of Ca^{2+} by mitochondria. Nevertheless, the ADP-induced increase in $[Ca^{2+}]_m$ may be ascribed in part to other mechanisms that we explored. Our experiments performed with RR indicate that the ADP-induced Ca^{2+} flux through the CU cannot explain the phenomenon. The NCE was not active in the Na^+-free buffer as verified by the NCE blocker CGP 37157. However, as there are currently no known blockers for Na^+-independent Ca^{2+} exchange (NICE) such as Ca^{2+}/H^+ (CHE), it is not possible to exclude a decrease in Ca^{2+} efflux through NICE during state 3 respiration as an alternative explanation for the net increase of Ca^{2+} flux into the matrix ($J_{net} = J_{CU} - J_{NICE}$) that causes the increase in $[Ca^{2+}]_m$. Because Ca^{2+} efflux through the NICE is dependent on both ΔpH ($[H^+]_e - [H^+]_m$) and $\Delta[Ca^{2+}]$ ($[Ca^{2+}]_m - [Ca^{2+}]_e$) (20,48), we would not expect a major change in Ca^{2+} efflux through the NICE during state 3 respiration, since $\Delta[Ca^{2+}]$ increases (Fig. 4) and ΔpH decreases (Fig. 7 *C*).

Another possible factor for the ADP-induced increase in $[Ca^{2+}]_m$ is the change in pH upon ADP addition. During state 3 respiration, pH_m decreases, albeit slightly (Fig. 7 *C*), due to influx of protons through the F_1F_0-ATPase (49). This transient acidification might affect the K_d between indo-1 and Ca^{2+} (50). However, the measured pH change was minimal (0.03 pH unit) and the reported changes in K_d were measured with a ΔpH of 1 pH unit. We expected the effect of ΔpH on $[Ca^{2+}]_m$ to be minimal in this study because of 1), the small change in pH_m, 2), the difference in $[Ca^{2+}]_m$ after ADP addition in the presence of low buffer P_i (no significant change in pH compared to control; data not shown), and 3), the increase in $[Ca^{2+}]_m$ after ADP addition in the presence of OMN (no significant change in pH on ADP addition; data not shown). Finally, the ADP-induced increase in $[Ca^{2+}]_m$ could be due to an alteration in Ca^{2+} buffering capacity by TCA cycle intermediates, which can bind to Ca^{2+} as well (51).

Changes in $[Ca^{2+}]_m$ and mitochondrial bioenergetics

These experiments did not show significant changes in mitochondrial bioenergetics when $CaCl_2$ was added to the buffer except for small increases in respiration in states 2 and 4, and only after 25 μM $CaCl_2$. Possible explanations for the increased resting-state respiration are opening of Ca^{2+}-dependent K^+ channels (31,52) or proton cycling through the putative NICE (48). In a previous study (53), in which respiration was measured in permeabilized cardiac cells, it was reported that adding $CaCl_2$ increased state 2 respiration, but decreased state 3 respiration. However, other studies report that an increase in $[Ca^{2+}]_m$ is associated with an increase in state 3 as well as state 2 respiration (5,54,55). In many of these studies, though, higher concentrations of $CaCl_2$ might have induced a large increase in respiration due to other factors, such as mPTP opening. In this study, irreversible mPTP opening did not occur, as there was no decrease in $\Delta\Psi_m$ at the highest $[Ca^{2+}]_m$ observed with ADP. The small increase in O_2 consumption on $CaCl_2$ addition was not accompanied by other changes in bioenergetics, indicating that any slight uncoupling effect of Ca^{2+} could easily be corrected by increasing TCA cycle activity.

Many studies have shown a correlation between mitochondrial NADH and $[Ca^{2+}]_m$ (1–3,6). A possible explanation for the lack of an increase in NADH with increased $[Ca^{2+}]_m$ is that the highest $[Ca^{2+}]_m$ only just reached the $K_{0.5}$ for activation of TCA cycle dehydrogenases of ~1 μM (55,56) during state 3 respiration, a period in which there is much fluctuation in bioenergetics. Other studies also

question the role of Ca^{2+} in activation of NADH-producing dehydrogenases (57,58). Although these studies did not disprove the hypothesis of Ca^{2+} activation of TCA dehydrogenases, they did ascribe the changes in bioenergetics at least in part to other mechanisms (e.g., Mg^{2+} and ADP/ATP ratio), indirectly altered by Ca^{2+}.

That an increase in $[Ca^{2+}]_m$ can activate TCA dehydrogenases in the matrix to enhance respiration was proposed long ago (55,56). Our study provides an alternative hypothesis to the correlation between work load (changes in NADH/NAD^+) and $[Ca^{2+}]_m$. We clearly observed an increase in $[Ca^{2+}]_m$ due to activation of oxidative phosphorylation with addition of ADP, and we believe this is due in part to a decrease in matrix Ca^{2+} buffering capacity of ADP versus ATP. It is conceivable that an increase in $[Ca^{2+}]_m$ is a result of enhanced phosphorylation-induced respiration, rather than enhanced respiration being a result of increased $[Ca^{2+}]_m$. Our study was not designed to disprove or prove the hypothesis of Ca^{2+} and its role in the regulation of mitochondrial bioenergetics; however, this alternative hypothesis should be further explored.

$[Ca^{2+}]_m$ and mitochondrial pH

Matrix pH was not significantly affected by increased $[Ca^{2+}]_m$. It was anticipated that $[Ca^{2+}]_m$ would compete with protons for binding with ATP, ADP, and P_i, and result in matrix acidification, just as acidification results in an increase in Ca^{2+} through buffering pathways (59). The amount of protons that dissociate from these buffering sites, when these sites bind to Ca^{2+}, apparently can be sufficiently buffered in the matrix to maintain pH. We observed that $[H^+]_m$ varies between 10 and 100 nM (pH between 7 and 8), which is about one order of magnitude lower than the changes in $[Ca^{2+}]_m$ in this study. This indicates a higher matrix buffering capacity for protons than for Ca^{2+}. Apparently the increase in $[Ca^{2+}]_m$ is insufficient to produce a significant decrease in the H^+ buffering capacity of the matrix. Otherwise, it is likely that an increase in proton expulsion coupled to electron transfer corrected for this increase in $[H^+]_m$, as respiration was slightly increased by $CaCl_2$ addition. We have shown in preliminary experiments (unblocked NCE) that pH decreases with the addition of higher $[CaCl_2]$ (50 or 100 μM) (J. Haumann, A. Camara, and D. Stowe, unpublished observations). This decrease in pH was not blocked by cyclosporin A, an mPTP inhibitor, indicating that mPTP opening did not cause the acidification.

SUMMARY AND CONCLUSIONS

To our knowledge, the up to twofold increase in $[Ca^{2+}]_m$ during oxidative phosphorylation under conditions of blocked CU and inactive NCE has not been reported previously. This study demonstrates the importance of changes in ADP phosphorylation on matrix free $[Ca^{2+}]$ and suggests a change in matrix buffering of Ca^{2+} or release of matrix stores of Ca^{2+} as possible mechanisms for the ADP-induced increase in $[Ca^{2+}]_m$. This observed increase may be dependent on buffer conditions and the different binding constants of Ca^{2+} to ATP, ADP, P_i, and matrix proteins. Changes in redox state, matrix pH, buffer $[P_i]$, and $[Mg^{2+}]_m$, did not alter $[Ca^{2+}]_m$. Activation of the CU, and contraction of the matrix volume by ADP did not appear to account substantially for this effect of ADP. The conventional postulation is that increased $[Ca^{2+}]_m$ enhances respiration via NADH-linked substrates; we show, alternatively, that ADP-induced stimulation of respiration enhances $[Ca^{2+}]_m$. Computer modeling (23) of the dynamics of Ca^{2+} flux and mitochondrial buffering mechanisms will help to confirm our findings, or to iteratively delineate the relative importance of each of the several proposed mechanisms that may modulate $[Ca^{2+}]_m$ between states 3 and 4.

The important and dependent relationship between $[Ca^{2+}]_m$ and [ADP], $[P_i]$, and [ATP] should lead to a reexamination of the relationship between $[Ca^{2+}]_m$ and control of respiration. Although increased $[Ca^{2+}]_m$ slightly enhanced respiration in states 2 and 4 (NCE blocked), the increase in $[Ca^{2+}]_m$ via reduced binding in the matrix during state 3 respiration did not enhance respiration. We could not demonstrate any Ca^{2+}-induced changes in $\Delta\Psi_m$ or NADH, but we found a small decrease in RCI, indicating slight uncoupling. The evidence that $\Delta\Psi_m$ and NADH were not different in the OMN and CATR groups suggests that the changes observed resulted from an altered buffering effect due to differences in the ADP and ATP concentrations or to release of Ca^{2+} from stores, and less from increased Ca^{2+} influx through stimulation of the CU, or decreased Ca^{2+} efflux through NCE.

SUPPORTING MATERIAL

One table, three figures, equations, and references are available at http://www.biophysj.org/biophysj/supplemental/S0006-3495(10)00619-3.

We thank Runa Patel, Mohammed Aldakkak, Kalyan C. Vinnakota, and Matthew R. Vernon for providing assistance in some experiments and for participating in many useful discussions.

This research was supported by grants from the National Institutes of Health (HL095122 to R.K.D. and A.K.S.C., HL089514 to D.F.S., and HL094317 to D.A.B.), and the American Heart Association (0855940G to D.F.S. and 08564N to R.K.D.).

REFERENCES

1. Brandes, R., and D. M. Bers. 1997. Intracellular Ca^{2+} increases the mitochondrial NADH concentration during elevated work in intact cardiac muscle. *Circ. Res.* 80:82–87.
2. Brandes, R., and D. M. Bers. 2002. Simultaneous measurements of mitochondrial NADH and Ca^{2+} during increased work in intact rat heart trabeculae. *Biophys. J.* 83:587–604.

3. McCormack, J. G., A. P. Halestrap, and R. M. Denton. 1990. Role of calcium ions in regulation of mammalian intramitochondrial metabolism. *Physiol. Rev.* 70:391–425.
4. Nguyen, M. H., S. J. Dudycha, and M. S. Jafri. 2007. Effect of Ca^{2+} on cardiac mitochondrial energy production is modulated by Na^{+} and H^{+} dynamics. *Am. J. Physiol. Cell Physiol.* 292:C2004–C2020.
5. Rossi, C. S., and A. L. Lehninger. 1964. Stoichiometry of respiratory stimulation, accumulation of Ca^{++} and phosphate, and oxidative phosphorylation in rat liver mitochondria. *J. Biol. Chem.* 239:3971–3980.
6. Territo, P. R., V. K. Mootha, …, R. S. Balaban. 2000. Ca^{2+} activation of heart mitochondrial oxidative phosphorylation: role of the F_0/F_1-ATPase. *Am. J. Physiol. Cell Physiol.* 278:C423–C435.
7. Bernardi, P. 1999. Mitochondrial transport of cations: channels, exchangers, and permeability transition. *Physiol. Rev.* 79:1127–1155.
8. Brookes, P. S., Y. Yoon, …, S. S. Sheu. 2004. Calcium, ATP, and ROS: a mitochondrial love-hate triangle. *Am. J. Physiol. Cell Physiol.* 287:C817–C833.
9. Duchen, M. R. 2000. Mitochondria and calcium: from cell signalling to cell death. *J. Physiol.* 529:57–68.
10. Gunter, T. E., K. K. Gunter, …, C. E. Gavin. 1994. Mitochondrial calcium transport: physiological and pathological relevance. *Am. J. Physiol.* 267:C313–C339.
11. O'Rourke, B., S. Cortassa, and M. A. Aon. 2005. Mitochondrial ion channels: gatekeepers of life and death. *Physiology (Bethesda).* 20:303–315.
12. Argaud, L., O. Gateau-Roesch, …, M. Ovize. 2005. Postconditioning inhibits mitochondrial permeability transition. *Circulation.* 111: 194–197.
13. Bopassa, J. C., D. Vandroux, …, R. Ferrera. 2006. Controlled reperfusion after hypothermic heart preservation inhibits mitochondrial permeability transition-pore opening and enhances functional recovery. *Am. J. Physiol. Heart Circ. Physiol.* 291:H2265–H2271.
14. Feng, J., E. Lucchinetti, …, M. Zaugg. 2005. Isoflurane postconditioning prevents opening of the mitochondrial permeability transition pore through inhibition of glycogen synthase kinase 3β. *Anesthesiology.* 103:987–995.
15. Halestrap, A. P., S. J. Clarke, and S. A. Javadov. 2004. Mitochondrial permeability transition pore opening during myocardial reperfusion–a target for cardioprotection. *Cardiovasc. Res.* 61:372–385.
16. Hausenloy, D. J., M. R. Duchen, and D. M. Yellon. 2003. Inhibiting mitochondrial permeability transition pore opening at reperfusion protects against ischaemia-reperfusion injury. *Cardiovasc. Res.* 60:617–625.
17. Nishihara, M., T. Miura, …, K. Shimamoto. 2007. Modulation of the mitochondrial permeability transition pore complex in GSK-3β-mediated myocardial protection. *J. Mol. Cell. Cardiol.* 43:564–570.
18. Gunter, T. E., and D. R. Pfeiffer. 1990. Mechanisms by which mitochondria transport calcium. *Am. J. Physiol.* 258:C755–C786.
19. Brand, M. D. 1985. Electroneutral efflux of Ca^{2+} from liver mitochondria. *Biochem. J.* 225:413–419.
20. Gunter, T. E., J. H. Chace, …, K. K. Gunter. 1983. Mechanism of sodium independent calcium efflux from rat liver mitochondria. *Biochemistry.* 22:6341–6351.
21. Rottenberg, H., and M. Marbach. 1990. The Na^{+}-independent Ca^{2+} efflux system in mitochondria is a $Ca^{2+}/2H^{+}$ exchange system. *FEBS Lett.* 274:65–68.
22. Wingrove, D. E., J. M. Amatruda, and T. E. Gunter. 1984. Glucagon effects on the membrane potential and calcium uptake rate of rat liver mitochondria. *J. Biol. Chem.* 259:9390–9394.
23. Dash, R. K., F. Qi, and D. A. Beard. 2009. A biophysically based mathematical model for the kinetics of mitochondrial calcium uniporter. *Biophys. J.* 96:1318–1332.
24. Dash, R. K., and D. A. Beard. 2008. Analysis of cardiac mitochondrial Na^{+}-Ca^{2+} exchanger kinetics with a biophysical model of mitochondrial Ca^{2+} handling suggests a 3:1 stoichiometry. *J. Physiol.* 586:3267–3285.
25. Litsky, M. L., and D. R. Pfeiffer. 1997. Regulation of the mitochondrial Ca^{2+} uniporter by external adenine nucleotides: the uniporter behaves like a gated channel which is regulated by nucleotides and divalent cations. *Biochemistry.* 36:7071–7080.
26. Chalmers, S., and D. G. Nicholls. 2003. The relationship between free and total calcium concentrations in the matrix of liver and brain mitochondria. *J. Biol. Chem.* 278:19062–19070.
27. Michailova, A., and A. McCulloch. 2001. Model study of ATP and ADP buffering, transport of Ca^{2+} and Mg^{2+}, and regulation of ion pumps in ventricular myocyte. *Biophys. J.* 81:614–629.
28. Grynkiewicz, G., M. Poenie, and R. Y. Tsien. 1985. A new generation of Ca^{2+} indicators with greatly improved fluorescence properties. *J. Biol. Chem.* 260:3440–3450.
29. Chance, B., P. Cohen, …, B. Schoener. 1962. Intracellular oxidation-reduction states in vivo. *Science.* 137:499–508.
30. Aldakkak, M., D. F. Stowe, …, A. K. S. Camara. 2010. Mitochondrial matrix K^{+} flux independent of large conductance Ca^{2+} activated K^{+} channel opening. *Am. J. Physiol. Cell Physiol.* 298:C530–C541.
31. Heinen, A., A. K. Camara, …, D. F. Stowe. 2007. Mitochondrial Ca^{2+}-induced K^{+} influx increases respiration and enhances ROS production while maintaining membrane potential. *Am. J. Physiol. Cell Physiol.* 292:C148–C156.
32. Riess, M. L., L. G. Kevin, …, D. F. Stowe. 2005. Anesthetic preconditioning: the role of free radicals in sevoflurane-induced attenuation of mitochondrial electron transport in Guinea pig isolated hearts. *Anesth. Analg.* 100:46–53.
33. Bradford, M. M. 1976. A rapid and sensitive method for the quantitation of microgram quantities of protein utilizing the principle of protein-dye binding. *Anal. Biochem.* 72:248–254.
34. McCormack, J. G., H. M. Browne, and N. J. Dawes. 1989. Studies on mitochondrial Ca^{2+}-transport and matrix Ca^{2+} using fura-2-loaded rat heart mitochondria. *Biochim. Biophys. Acta.* 973:420–427.
35. Wan, B., K. F. LaNoue, …, R. C. Scaduto, Jr. 1989. Regulation of citric acid cycle by calcium. *J. Biol. Chem.* 264:13430–13439.
36. Nicholls, D. G. 1978. The regulation of extramitochondrial free calcium ion concentration by rat liver mitochondria. *Biochem. J.* 176:463–474.
37. Nicholls, D. G., and I. D. Scott. 1980. The regulation of brain mitochondrial calcium-ion transport. The role of ATP in the discrimination between kinetic and membrane-potential-dependent calcium-ion efflux mechanisms. *Biochem. J.* 186:833–839.
38. Zoccarato, F., and D. Nicholls. 1982. The role of phosphate in the regulation of the independent calcium-efflux pathway of liver mitochondria. *Eur. J. Biochem.* 127:333–338.
39. McGivan, J. D., K. Grebe, and M. Klingenberg. 1971. On the coupling between the transport of phosphate and adenine nucleotides in rat liver mitochondria. *Biochem. Biophys. Res. Commun.* 45:1533–1541.
40. Jorgensen, A. O., A. C. Shen, …, K. P. Campbell. 1993. The Ca^{2+}-release channel/ryanodine receptor is localized in junctional and corbular sarcoplasmic reticulum in cardiac muscle. *J. Cell Biol.* 120:969–980.
41. Chan, S. H., and R. L. Barbour. 1983. Adenine nucleotide transport in hepatoma mitochondria. Characterization of factors influencing the kinetics of ADP and ATP uptake. *Biochim. Biophys. Acta.* 723: 104–113.
42. Klingenberg, M. 2008. The ADP and ATP transport in mitochondria and its carrier. *Biochim. Biophys. Acta.* 1778:1978–2021.
43. Pfaff, E., and M. Klingenberg. 1968. Adenine nucleotide translocation of mitochondria. 1. Specificity and control. *Eur. J. Biochem.* 6:66–79.
44. Coty, W. A., and P. L. Pedersen. 1974. Phosphate transport in rat liver mitochondria. Kinetics and energy requirements. *J. Biol. Chem.* 249:2593–2598.
45. Stappen, R., and R. Kramer. 1994. Kinetic mechanism of phosphate/phosphate and phosphate/OH^{-} antiports catalyzed by reconstituted phosphate carrier from beef heart mitochondria. *J. Biol. Chem.* 269:11240–11246.

46. Wohlrab, H. 1986. Molecular aspects of inorganic phosphate transport in mitochondria. *Biochim. Biophys. Acta.* 853:115–134.

47. Vignais, P. V., P. M. Vignais, and J. Doussiere. 1975. Functional relationship between the ADP/ATP-carrier and the F_1-ATPase in mitochondria. *Biochim. Biophys. Acta.* 376:219–230.

48. Gunter, K. K., M. J. Zuscik, and T. E. Gunter. 1991. The Na^+-independent Ca^{2+} efflux mechanism of liver mitochondria is not a passive $Ca^{2+}/2H^+$ exchanger. *J. Biol. Chem.* 266:21640–21648.

49. Fillingame, R. H. 1997. Coupling H^+ transport and ATP synthesis in F_1F_0-ATP synthases: glimpses of interacting parts in a dynamic molecular machine. *J. Exp. Biol.* 200:217–224.

50. Baker, A. J., R. Brandes, …, M. W. Weiner. 1994. Protein and acidosis alter calcium-binding and fluorescence spectra of the calcium indicator indo-1. *Biophys. J.* 67:1646–1654.

51. Ranby, M., T. Gojceta, …, T. L. Lindahl. 1999. Isocitrate as calcium ion activity buffer in coagulation assays. *Clin. Chem.* 45:1176–1180.

52. Heinen, A., A. Winning, …, N. C. Weber. 2008. The regulation of mitochondrial respiration by opening of mK_{Ca} channels is age-dependent. *Eur. J. Pharmacol.* 578:108–113.

53. Tsokos, J., and S. Bloom. 1977. Effects of calcium on respiration and ATP content of isolated, leaky, heart muscle cells. *J. Mol. Cell. Cardiol.* 9:823–836.

54. Roman, I., A. Clark, and P. D. Swanson. 1981. The interaction of calcium transport and ADP phosphorylation in brain mitochondria. *Membr. Biochem.* 4:1–9.

55. McCormack, J. G., and R. M. Denton. 1980. Role of calcium ions in the regulation of intramitochondrial metabolism. Properties of the Ca^{2+}-sensitive dehydrogenases within intact uncoupled mitochondria from the white and brown adipose tissue of the rat. *Biochem. J.* 190:95–105.

56. Denton, R. M., J. G. McCormack, and N. J. Edgell. 1980. Role of calcium ions in the regulation of intramitochondrial metabolism. Effects of Na^+, Mg^{2+} and ruthenium red on the Ca^{2+}-stimulated oxidation of oxoglutarate and on pyruvate dehydrogenase activity in intact rat heart mitochondria. *Biochem. J.* 190:107–117.

57. Qi, F., X. Chen, and D. A. Beard. 2008. Detailed kinetics and regulation of mammalian NAD-linked isocitrate dehydrogenase. *Biochim. Biophys. Acta.* 1784:1641–1651.

58. Hak, J. B., J. H. Van Beek, …, N. Westerhof. 1993. Mitochondrial dehydrogenase activity affects adaptation of cardiac oxygen consumption to demand. *Am. J. Physiol.* 264:H448–H453.

59. Gambassi, G., R. G. Hansford, …, M. C. Capogrossi. 1993. Effects of acidosis on resting cytosolic and mitochondrial Ca^{2+} in mammalian myocardium. *J. Gen. Physiol.* 102:575–597.